Development of a Small Animal SPECT Imager with LYSO Scintillator Arrays and PSPMTs

Qiushi Zhang[1,2]
[1]Institute for Drug and Instrument Control of PLA
Beijing, China
zhangqsh@pku.edu.cn

Suying Li[2], Zhaoheng Xie[2], Yanye Lu[2], Kun Yang[2], Qiushi Ren[2]
[2]Department of Biomedicine and Engineering
Peking University
Beijing, China
lisuying90@163.com

***Abstract*—We describe a small animal SPECT imager based on scintillation crystal arrays and position sensitive photomultiplier tube (PSPMT). This SPECT detector consists of a cerium doped lutetium-yttrium oxyorthosilicate (LYSO) scintillation crystal (22 × 22 pixel array, 2 mm × 2 mm × 3 mm pixel size), a H8500c PSPMT (Hamamatsu Photonics Co., Ltd., Shizuoka Prefecture, Japan), and a parallel hole collimator (Nuclear Fields Pty. Ltd, St. Marys, Australia). The detector design, electronic setup and image correction method are presented. Conical phantom study and animal experiment (BALB/C male nude mice, 16 week, 20g) were performed for the uniformity correction evaluation and imaging performance test respectively. The preliminary results demonstrate that this SPECT imager can achieve the small animal whole body imaging effectively and thus be one of the modalities of our future multimodality imaging system. The feasibility that LYSO crystal can substitute NaI(TI) for SPECT imager development is also validated..** *(Abstract)*

***Index Terms*—animal imaging, image correction, single photon emission computed tomography, ^{99m}Tc-3PRG2, tumor.**

I. INTRODUCTION

Nuclear medicine imaging (NMI) techniques, such as positron emission tomography (PET) and single-photon emission computed tomography (SPECT), are playing an increasingly important role in gaining insights into pathological processes in preclinical studies [1]. Compared with PET, SPECT has several characteristics and thus is more practical because of its potential for higher spatial resolution [2], a wider range of radionuclides, and the use of multiple-label molecular probes that provide the capability to investigate complicated molecular events in vivo [3, 4]. Over the past decade, SPECT imaging has been applied extensively in cardiology, neurology, oncology and drug discovery and evaluation [3]. The growth in these nuclear imaging applications has motivated both academic and industrial development of SPECT systems that are designed specifically for small-animal imaging.

A SPECT imaging scanner consists of a collimator, scintillation crystal, photoelectric detector, electrical readout modules, and image processing/display devices. Since the Anger camera was first designed in the last century [5], the design scheme, scintillation crystal plus PMTs, came to dominate the field of gamma-ray detector design. Scintillators are the first thing that should be carefully considered when gamma-ray detectors are designed. Currently, the most widely used scintillation crystals for SPECT include thallium-doped sodium iodide (NaI(TI)), bismuth germinate (BGO) and cerium doped lutetium oxyorthosilicate (LSO). NaI(TI) remains the most common scintillator material and has been used by a number of investigators to build many typical SPECT prototypes, e.g. A-SPECT developed by University of North Carolina [6], U-SPECT by the Medicine Centre of Utrecht University [7], nanoSPECT by BIOSCAN [8], FastSPECT-I and FastSPECT-II by Arizona University [9, 10]. NaI(TI) crystal has high light output and is possible to reliably produce large crystals. However, the hygroscopic property exhibited by NaI(TI) is an undesirable trait in a gamma-ray detector design. BGO crystals have a long decay time (~300ns) and thus are replaced by LSO that surpasses BGO on light output and decay time. Nevertheless, the high melting point of LSO crystal make it hard to grow. Cerium doped lutetium-yttrium oxyorthosilicate (LYSO) scintillation crystal, which has the similar properties as LSO, is much easier to produce due to the lower melting point and less expensive ingredients required [11, 12].

Our objective is to develop a SPECT imager for our multimodality imaging system. In the current study, we describe a small animal SPECT imager based on LYSO scintillation crystal arrays and position sensitive photomultiplier tube (PSPMT). The detector design and electronic setup for data acquisition are presented. Spatial resolution test was performed and a uniformity correction method was developed in order to improve the detector performance. We characterized this performance before and after uniformity correction and thus the correction effect was evaluated. Animal imaging experiment was also performed to evaluate the performance of the SPECT imaging system preliminarily.

978-1-4799-1467-8/13/$31.00 ©2013 IEEE

II. System Design

A. Detector Description

The small gamma camera consists of a parallel-hole lead collimator (Nuclear Fields Pty. Ltd, St. Marys, Australia), a LYSO scintillation crystal array (22 × 22 pixel array, 2mm × 2mm × 3mm pixel size, Yibo Crystal Technology Co. Ltd, Shanghai, China), a PSPMT (H8500c, Hamamatsu Photonics Co. Ltd., Shizuoka Prefecture, Japan), and subtractive-resistive readout electronics. The parallel-hole collimator measures 34.8 mm thick, with 1.5-mm diameter cylindrical holes and septa thickness of 0.2mm. The Hamamatsu H8500c PSPMT coupled to the scintillation crystal array has an active area of 49 × 49 mm^2 with high packing density and small dead space and can provide unusually high resolution in imaging. It is equipped with 64 (8 × 8 matrix) anode pads and a 12-stage dynode with bialkali photocathodes. It has a spectrum response range of 300 nm ~ 650 nm with the peak wavelength of 400 nm. The detectors are enclosed in aluminium housings (Fig.1). The SPECT imager consists of two detectors mounted face to face in a rotating gantry. The two detectors are shifted in the axial direction with their active areas overlapped to obtain an extended field of view (FOV).

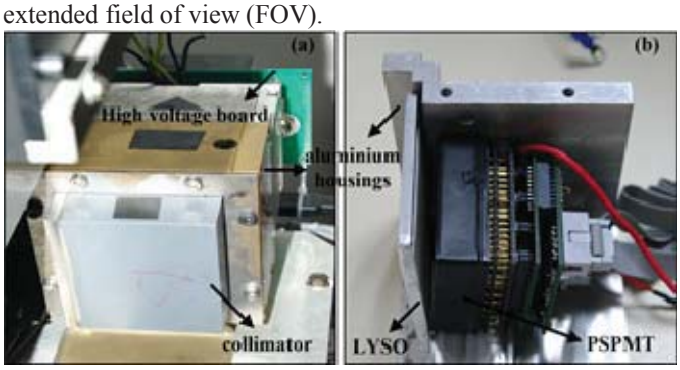

Fig. 1. Photograph of the gamma detector (a) and its interior structure (b).

B. Electronic Setup

Schematic block diagram of the electronic setup is shown in Fig.2. The electronics of this SPECT imager consist of high voltage board, readout circuitry and ADC data acquisition board. A ~1000 V negative voltage is generated from high voltage board to supply H8500 PSPMT. The readout circuitry is contained on a printed circuit board that is attached to each PSPMT. The signals from the 64 anodes of the PSPMT are de-coupled and combined into 16 stripe readout channels and then processed by a resistive chain to produce four signals (X+, X-, Y+, Y-). These signals reflect the position information of a gamma-ray event. Meanwhile, the energy signal is obtained from adding of the signals of all the anode pads of PSPMT. Then the five signals (position and energy signals), after having been preamplified, are fed to ADC data acquisition board which was developed by our group. A digitized output is then generated via A/D transformation and acquired by a host computer.

C. Image Correction

Image correction was performed using position mapping and uniformity correction. We developed a position mapping algorithm that is based on connected regional recognition using digital image processing techniques. This algorithm can produce a mapping look-up table (LUT) that defines the matching relationship between the signal location of a detected event and the corresponding detector pixel location. Uniformity correction (or flood correction) is performed using a corresponding LUT of correction coefficients after position mapping and thus could further improve the image quality. We do not perform scatter calibration and attenuation correction in our imaging system because the scatter calibration that is often used in PET imaging [13] is not critical in SPECT since the lower energy of 140keV disregards the influence of Compton scattering. In addition, the attenuation correction, as mentioned by many authors [14, 15], might not be a major issue in small-animal SPECT imaging studies.

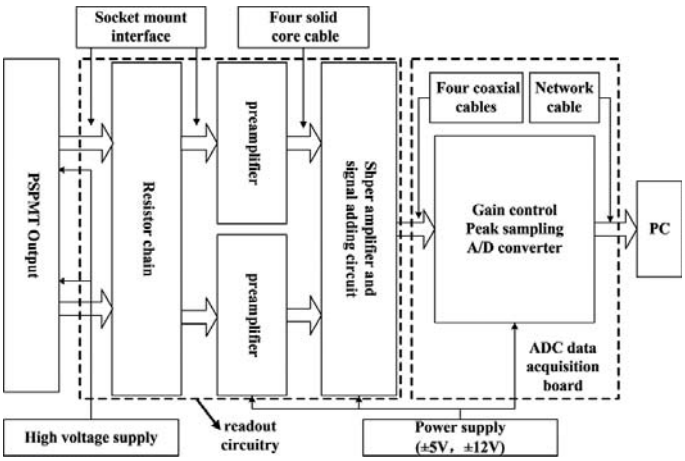

Fig. 2. Schematic block diagram of the electronic setup of the SPECT imager.

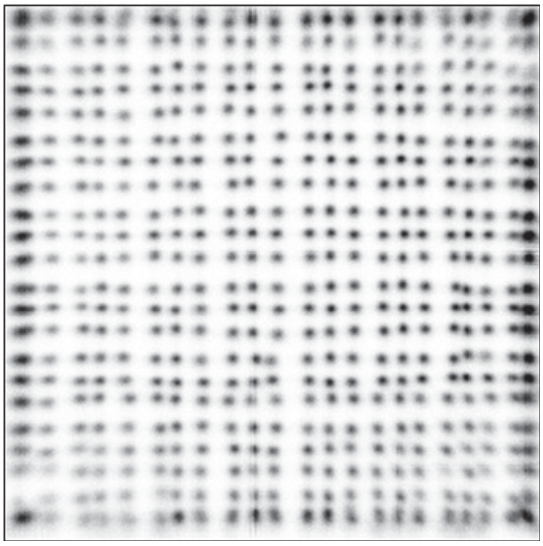

Fig. 3. Raw image of the pixelated crystal scintillators (22 × 22 matrix).

III. Experimental Method

A. Spatial Resolution Test

The spatial resolution was measured using two parallel capillary tubes (inner diameter: 2mm) which were filled with 1mCi ^{99m}Tc and positioned 50 mm from the face of the collimator. These two line sources with 4mm, 5mm, 6mm and 7mm spacing were scanned respectively in the step-and-shoot mode from 120 directions over 360°. The acquisition time was 60 s. Line test was then performed on the transaxial section of reconstructed images in order to judge if the two line source can be resolved.

B. Image Correction Test

We evaluated the scanner performance for uniformity before and after correction. As shown in Fig.3, the raw image obtained with the PSPMTs exhibited crystal location distortion, with some points overlapping one another because of the non-linear and non-uniform spatial response from the PSPMT system. A phantom (a conical bottle filled with ^{99m}Tc, Fig. 4) was used to evaluate the correction of the reconstructed image data, but it left an air bubble. The conical bottle with an air bubble served two purposes. First, the conical bottle is spatially symmetrical in shape, thus ensuring a uniform distribution of the pharmaceutical concentration inside. Second, the conical bottle was used to validate the tomographic image because it varies in diameter from the top to the bottom of the bottle. In addition, the air bubble left inside introduces some variation between the slices in the reconstructed images; therefore, it can be used to verify the validity of the correction method. The projection data were acquired for 90 seconds in the step-and-shoot mode from 120 directions over 360°. More details about the correction algorithm were described in Ref. [16].

Fig. 4. The conical phantom (bottom diameter: 300 mm, height: 600 mm) used for the reconstruction image evaluation.

C. Animal Imaging

This study was performed with the approval of the local ethical committee and the experimental protocol was completely approved by the Animal Centre of Peking University. BALB/C male nude mice, weighting 20 g, were inoculated subcutaneously with Hep3B human hepatoma cells (6.25×10^7 cells per mouse) into the flank area of the right shoulder. Two weeks after the xenograft tumor inoculation, when the tumors were 3mm~4 mm in diameter (area: ~12 mm^2), the mice were ready to perform imaging test. Eachamouse was then intravenously injected with 37.0 MBq ^{99m}Tc-3PRG2 (3PRGD2=PEG4-E[PEG4-c(RGDfK)]2) [17]. After a 50-min uptake period, the mouse was subject to the anesthesia with 2.50% isoflurane in oxygen for inducing anesthesia and then 1.00% isoflurane in oxygen for anesthesia maintenance. The mouse was covered by cotton in order to maintain its body temperature during the whole experimental procedure [18]. SPECT projection data were acquired in a step-and-shoot mode from 60 angles over 180° with the acquisition time of 20s per projection. The acquired projection data were reconstructed using ART.

IV. Preliminary Imaging Results

Fig. 5 shows the transaxial section of tomographic images of the line source phantom (top) and the corresponding line test profiles (bottom). The capillary tubes with >5 mm apart can be distinguished, which indicates a spatial resolution of ~2.5 mm. Fig. 6 (top) shows the serial axial slices from the conical phantom images, which were reconstructed from the projection data using ART without uniformity correction. The projection data were reconstructed again after the uniformity correction, and the air bubble can be clearly observed in the reconstructed images (Fig. 6, bottom). The integral uniformity values of the reconstructed SPECT images (Fig. 7) further validate the effectiveness of the correction method.

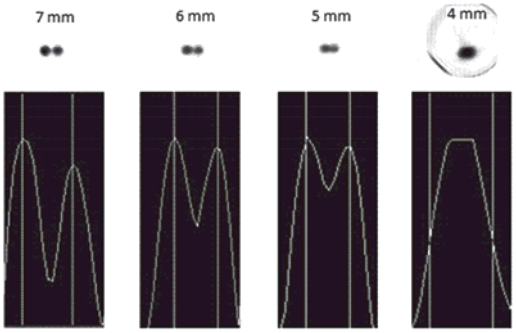

Fig. 5. Transaxial section of tomographic images of the line source phantom (top) and the corresponding line test profiles (bottom).

The SPECT images of xenograft tumor are shown in Fig. 8. Both of the transverse and sagittal image showed a higher radioactivity concentration in the tumor in the right shoulder. Moreover, it presents a good uniformity within the tumor area after detector calibration. Note that a higher uptake of ^{99m}Tc-3PRG2 was also observed in the liver and the abdominal viscera. The pharmaceuticals in these organs were metabolized by the kidney to the bladder together. A better control of pharmaceuticals metabolism time might help to reduce the high uptake in the abdominal viscera. Furthermore, inducing micturition for mice before experiment would eliminate high count rate of gamma ray event in the bladder. It is also worth noting that the event count rate in the background is not as low as expected ideally despite a clearly higher uptake of ^{99m}Tc-3PRG2 in the tumor cells. This is probably because the

intrinsic activity of LYSO crystal creates a background count rate since LYSO (or LSO) is abundant in radioactive ^{176}Lu naturally [19]. Further study are needed to investigate this issue quantitatively in order to further improve the SPECT imager performance.

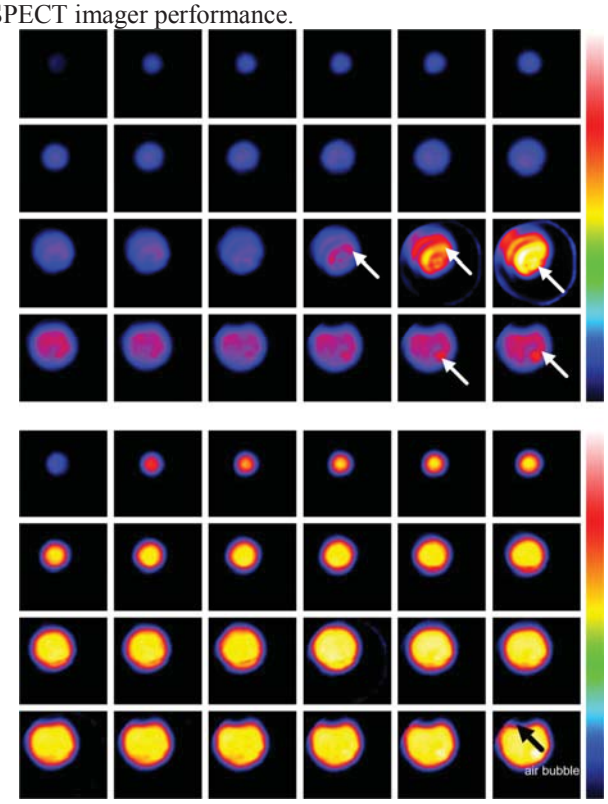

Fig. 6. Comparison between the representative axial slice images before (top) and after (bottom) the uniformity correction. The projection images were acquired for 120 directions over 360°. The acquisition time was 90 seconds for each direction. Twenty-four typical reconstructed images were selected to analyze the integral uniformity improvement after the uniformity correction. Note that the axial slice images (top), which were reconstructed from projection data without correction, still showed severe non-uniformities. The areas with high gray values in these slices are indicated (arrows).

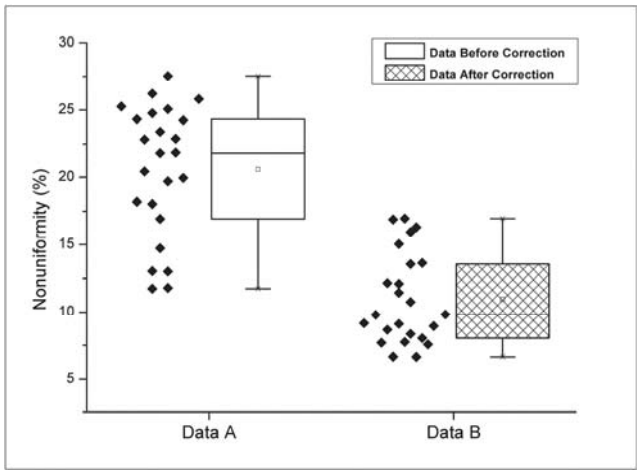

Fig. 7. Integral uniformity of the reconstructed SPECT images (see Fig.5) before (mean 20.56% ± 4.87) and after (mean 10.96% ± 3.38) the projection data correction.

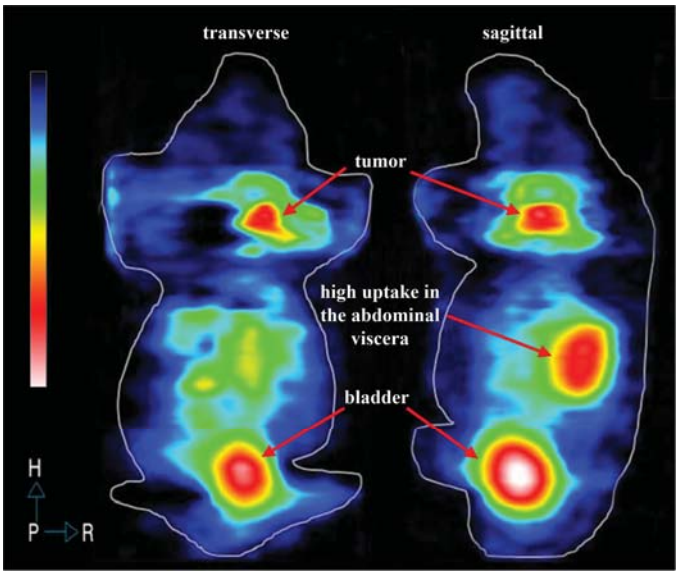

Fig. 8. Transverse (left) and sagittal (right) sections of 99mTc-3PRG2 SPECT image of BALB/C male nude mouse. Physiologic tracer uptake in tumor, abdominal viscera and bladder is marked.

V. Conclusion

We have presented the design and preliminary performance test of a SPECT imager based on LYSO scintillator and H8500 PSPMTs. Phantom study demonstrated that our compact gamma detector can achieve SPECT images with high uniformity. Animal experiment showed that the detector can provide a field of view that is sufficiently large for small animal whole body imaging. The spatial resolution is about 2.5 mm. Further performance measurement of this system is underway, including energy resolution, count rate capability and sensitivity test. In addition, the influence of background signals produced by the presence of the naturally occurring isotope ^{176}Lu should be investigated quantitatively in the future. We are also investigating the use of CdZnTe semiconductor and pinhole collimator to build a high performance SPECT imager.

References

[1] M. A. Pysz, S. S. Gambhir, and J. K. Willmann, "Molecular imaging: current status and emerging strategies," Clinical Radiology, vol. 65, pp. 500-516, 2010.

[2] C. M. Gomes, A. J. Abrunhosa, P. Ramos, and E. K. J. Pauwels, "Molecular imaging with SPECT as a tool for drug development," Advanced Drug Delivery Reviews, vol. 63, pp. 547-554, 6/19/ 2011.

[3] B. L. Franc, P. D. Acton, C. Mari, and B. H. Hasegawa, "Small-Animal SPECT and SPECT/CT: Important Tools for Preclinical Investigation," Journal of Nuclear Medicine, vol. 49, pp. 1651-1663, October 2008 2008.

[4] J. M. Park and S. S. Gambhir, "Multimodality Radionuclide, Fluorescence, and Bioluminescence Small-Animal Imaging," Proceedings of the IEEE, vol. 93, pp. 771-783, 2005.

[5] H. O. Anger, "2 Scintillation Camera," Review of Scientific Instrum., vol. 29, pp. 27-33, 1958.

[6] D. P. McElroy, L. R. MacDonald, F. J. Beekman, W. Yuchuan, B. E. Patt, J. S. Iwanczyk, et al., "Performance evaluation of A-SPECT: a high resolution desktop pinhole SPECT system for imaging small animals," Nuclear Science, IEEE Transactions on, vol. 49, pp. 2139-2147, 2002.

[7] F. J. Beekman and B. Vastenhouw, "Design and simulation of U-SPECT, an ultra-high resolution molecular imaging system," in Nuclear Science Symposium Conference Record, 2002 IEEE, 2002, pp. 792-796 vol.2.

[8] N. Schramm, C. Lackas, J. Hoppin, F. Forrer, and M. de Jong, "The nanoSPECT/CT: a high-sensitivity small-animal SPECT/CT with submillimeter spatial resolution," European Journal of Nuclear Medicine and Molecular Imaging, vol. 33, p. S117, 2006.

[9] Z. Liu, G. A. Kastis, G. D. Stevenson, H. H. Barrett, L. R. Furenlid, M. A. Kupinski, et al., "Quantitative Analysis of Acute Myocardial Infarct in Rat Hearts with Ischemia-Reperfusion Using a High-Resolution Stationary SPECT System," Journal of Nuclear Medicine, vol. 43, pp. 933-939, July 1, 2002 2002.

[10] L. R. Furenlid, D. W. Wilson, C. Yi-Chun, K. Hyunki, P. J. Pietraski, M. J. Crawford, et al., "FastSPECT II: a second-generation high-resolution dynamic SPECT imager," Nuclear Science, IEEE Transactions on, vol. 51, pp. 631-635, 2004.

[11] L. Qin, H. Li, S. Lu, D. Ding, and G. Ren, "Growth and characteristics of LYSO (Lu2(1−x−y)Y2xSiO5:Cey) scintillation crystals," Journal of Crystal Growth, vol. 281, pp. 518-524, 2005.

[12] D. Junwei, W. Yonggang, Z. Lijun, Z. Zhonghui, X. Zizhong, and W. XiaoLian, "Physical Properties of LYSO Scintillator for NN-PET Detectors," in Biomedical Engineering and Informatics, 2009. BMEI '09. 2nd International Conference on, 2009, pp. 1-5.

[13] C. Ju-Chieh, S. Blinder, A. Rahmim, and V. Sossi, "A Scatter Calibration Technique for Dynamic Brain Imaging in High Resolution PET," Nuclear Science, IEEE Transactions on, vol. 57, pp. 225-233, 2010.

[14] L. Bouwens, R. Van de Walle, J. Nuyts, M. Koole, Y. D'Asseler, S. Vandenberghe, et al., "Image-correction techniques in SPECT," Computerized medical imaging and graphics : the official journal of the Computerized Medical Imaging Society, vol. 25, pp. 117-126, 2001.

[15] M. Gombia, A. Tartari, M. Gambaccini, G. D. Domenico, D. Bollini, and A. D. Guerra, "Attenuation compensation for breast tissue in combined CT/SPECT devices dedicated to mammography," Nuclear Instruments and Methods in Physics Research Section A: Accelerators, Spectrometers, Detectors and Associated Equipment, vol. 497, pp. 150-156, 1/21/ 2003.

[16] Q. Zhang, Y. Lu, K. Yang, Q. Ren, “Position mapping and a uniformity correction method for small-animal SPECT based on connected regional recognition,” Nuclear Instruments and Methods in Physics Research Section A, vol. 704, pp. 1-6, March 2013.

[17] B. Jia, Z. Liu, Z. Zhu, J. Shi, X. Jin, H. Zhao, et al., "Blood Clearance Kinetics, Biodistribution, and Radiation Dosimetry of a Kit-Formulated Integrin αvβ3-Selective Radiotracer 99mTc-3PRGD2 in Non-Human Primates," Molecular Imaging and Biology, vol. 13, pp. 730-736, 2011/08/01 2011.

[18] B. J. Fueger, J. Czernin, I. Hildebrandt, C. Tran, B. S. Halpern, D. Stout, et al., "Impact of Animal Handling on the Results of 18F-FDG PET Studies in Mice," Journal of Nuclear Medicine, vol. 47, pp. 999-1006, June 2006 2006.

[19] J. S. Huber, W. W. Moses, W. F. Jones, and C. C. Watson, "Effect of 176Lu background on singles transmission for LSO-based PET cameras," Physics in medicine and biology, vol. 47, pp. 3535-3541, 10/ 2002.